11th Australasian Fluid Mechanics Conference
University of Tasmania, Hobart, Australia
14-18 December 1992

MODELLING OF A STEADY AND FULLY PULSED REATTACHING RADIAL JET

N.D AGNEW, D.G. ELVERY and K.BREMHORST

Department of Mechanical Engineering
University of Queensland
QLD 4072, AUSTRALIA

ABSTRACT

Numerical and experimental investigations were performed to characterise the steady and pulsed *R*adial *J*et *R*eattachment (RJR) flow fields. Comparisons between mean velocity fields predicted by computer modelling, flow visualisation and measurements obtained from laser Doppler anemometry techniques demonstrate good agreement for the steady and the developing pulsed jets.

A comparison of the turbulence characteristics for the steady RJR jet and the pulsating RJR jet along with their significance for potential industrial applications will also be presented. The k-ε model is shown to be deficient in predicting turbulence characteristics of the flow fields as they have multiple time scales.

The results obtained show that the turbulence intensity near the surface is enhanced when the frequency of pulsation exceeds a limiting value. The limiting frequency, above which reattachment does not occur, is presented along with its dependence on nozzle geometry and flow parameters.

NOTATION

b	Nozzle exit gap
C_p	Pressure coefficient, $\frac{p-p_\infty}{0.5\rho V_e^2}$
f	Pulse frequency (Hz)
k	Turbulent kinetic energy
p, p_∞	Local pressure, free stream pressure
r	Radial coordinate direction
r_o, r_R	End plate radius, reattachment radius
Re	Gap Reynolds number, $V_e b/\nu$
t	Time
u,v,w	Velocity fluctuations
U	Mean axial velocity component
V	Mean radial velocity component
V_e	Nozzle exit velocity
x	Axial coordinate direction from nozzle exit
X_p	Nozzle to surface distance
z	Axial coordinate direction from surface
ρ	Density
ε	Dissipation
ν	Kinematic viscosity
$\rho\overline{uv}$	Reynolds shear stress

INTRODUCTION

Mass and heat transfer operations are major energy consumers in industry. Preliminary studies into the operation of the Radial Jet Reattachment (RJR) nozzle have indicated (Page and Kiel, 1990) a substantial improvement in transfer rates as compared to normally impinging jets used for commercial convective drying. The basic configuration of the RJR nozzle, as developed at Texas A&M University, is of an axisymmetric radial jet above an infinite surface (Fig. 1). The increase in transfer rates is due to the higher turbulence within the flow as it reattaches onto the adjacent surface. The RJR nozzle is also able to establish a positive, negative or zero average surface pressure depending on exit geometry.

Entrainment of the surrounding fluid results in sub-atmospheric pressures beneath the nozzle, causing the initial radial flow to be deflected towards the surface forming an unstable reattachment ring. A finite time scale is involved in the establishment of the reattachment curtain leading to a large scale sweeping action of the flow field with associated changes in the transport characteristics. An aim of the present project is to determine the effect of flow pulsing on this mechanism.

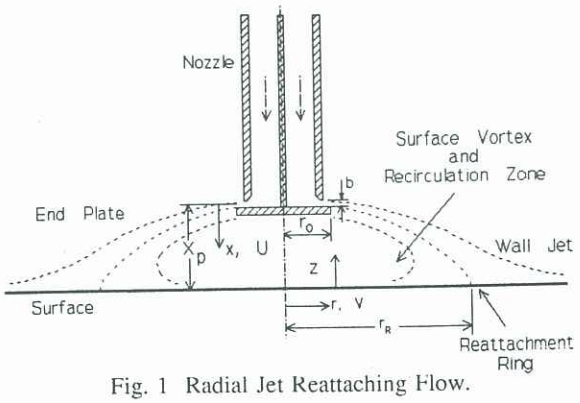

Fig. 1 Radial Jet Reattaching Flow.

APPARATUS AND PROCEDURES

The nozzle (Fig. 1), had a 25.7mm internal diameter with an end plate radius, r_o of 19.3mm. The radial gap, b was set to 0.5mm to ensure an ideal radial jet. The working fluid, air, had an exit velocity of up to 150 m/s corresponding to a gap Re of 4200. The plate distance, X_p was varied between 15mm and 40mm.

The pulse valve consisted of two counter-rotating

discs each with several perforations evenly spaced around their circumference. A variable speed gearbox was used, enabling control of the pulse frequency up to 50 Hz.

A pressure tapping in the impingement plate on the nozzle centreline and a micro-manometer were used for all pressure measurements.

Laser Doppler Anemometry (LDA)

A laser Doppler technique was chosen to measure the mean and fluctuating velocity components of the steady and pulsed reattaching fields. Being non-intrusive, it was well suited for the frequently reversing flow.

A TSI two component polarisation laser Doppler anemometer system was used with forward scatter and a shift frequency of 40 MHz. The intersection angle of the beams was 11.03°. An atomised water-glycerol mixture with a maximum particle diameter of 3.8 μm was used for seeding of the flow.

With a maximum available data validation rate of 10.4kHz per channel, sample and hold processing was implemented to ensure minimum velocity bias errors in the results obtained. The data density, defined as the ratio of the integral time scale of the flow to the inverse of the measurement data rate, was greater than 5, the value suggested for bias free results by Winter et al. (1991).

Flow Visualisation

Flow visualisation was achieved using a fine laser light sheet projected from a cylindrical lens illuminating the seeded flow field. Images were captured via digital video processing and high speed polaroid photography.

Numerical Computations

PHOENICS, a commercial finite difference code was used to compute the velocity field and turbulence characteristics by discretizing the Navier-Stokes equations and applying the k-ε turbulence model. The equations and model constants used were the same as those of Bremhorst and Flint (1988).

METHOD AND RESULTS

Steady Flow Characteristics

RJR flow field. The RJR flow issues from the nozzle in a radial direction but as noted above, due to entrainment is drawn downwards towards the surface. The jet forms a reattachment "curtain" under which is a large recirculation region (Fig. 1). This recirculation region contains what appears to be a toroidal vortex (Fig. 2), which is consistent with the predicted results of Fig. 3.

In the plane of the surface, the reattachment curtain develops a stagnation ring as distinct from a single stagnation point in a normally impinging jet. The

Fig. 2 RJR flow field visualisation.

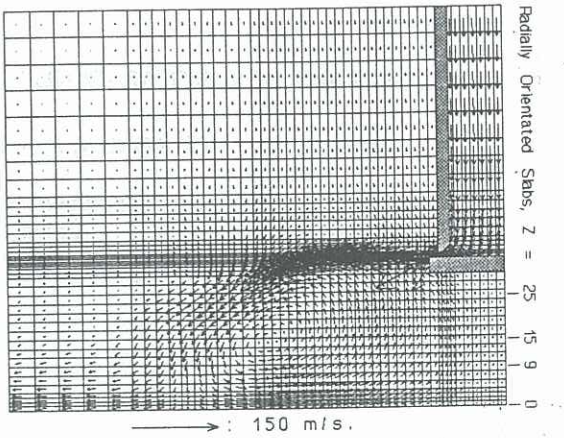

Fig. 3 Computed steady flow field.

position of this ring, r_R, is independent of the nozzle exit velocity, V_e but highly dependant on the nozzle to surface distance, X_p. The stagnation (or reattachment) ring has a finite thickness due to the high turbulence present and the instability of the curtain. This instability was evident in the form of "blowouts" caused by the build up of entrained fluid beneath the curtain. During blowouts, the flow loses its axisymmetry.

Further out in the flow beyond the stagnation ring, the flow settles down to a wall jet radiating outwards from the nozzle similar to a normally impinging jet flow.

Velocity measurement. These features of the flow can be seen in Fig. 4 and 5 for an X_p of 30mm. The plots show a comparison of the velocity components in the radial and axial directions between the numerically modelled and experimental results. Results were obtained from radially orientated slabs located 9, 15 and 25 mm from the surface and were normalised on V_e. A limitation was imposed on the proximity of the measurements to the surface by the finite intersection angle of the LDA beams.

As can be seen, the k-ε model accurately predicts the RJR flow field. The plots clearly indicate the existence of the recirculation region by the change in sign of the velocity components. The centre of the primary vortex is located at a radial distance of 2.75 r_o, the point at which the axial velocity component changes sign (Fig. 4). Past this point the velocity reaches a maximum at the centre of the main jet.

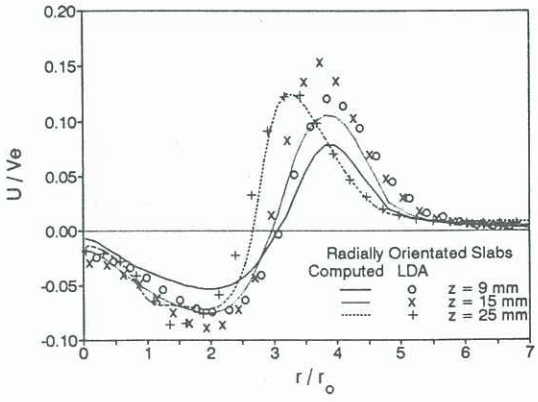

Fig. 4 Axial velocity profiles for steady flow.

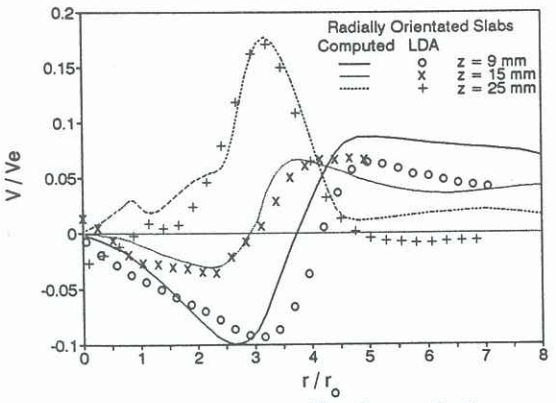

Fig. 5 Radial velocity profiles for steady flow.

The vortex can once again be seen from the radial velocity component curves (Fig. 5). The 9mm slab passes beneath the vortex centre as indicated by the position of the maximum negative velocity at a radius of 2.75 r_o. A zero velocity value at 2.75 r_o demonstrates that the 15mm slab passes near to the vortex centre itself. The maximum velocity in the 25mm slab is slightly displaced from the 2.75 r_o position due to its proximity to the main jet.

The kink exhibited at a radius of 1.5 r_o in both velocity curves (Fig. 4 and 5) for z = 25mm is caused by the entrained flow around the edge of the end plate.

Pulsed Flow Characteristics

Periodic pulsing of a flow produces higher levels of turbulence and hence higher transfer rates.

It was observed by Elvery (1991) and Agnew (1991) that there was some finite time scale involved in the jet reattachment onto the adjacent surface. At high frequencies of pulsation, the flow did not have time to reattach and stabilise, resulting in a highly irregular flow.

Limiting Frequency It has been found that the limiting frequency depends on the velocity and X_p (Fig. 6). The pressure at the surface on the axis of the nozzle was used to determine the extent of reattachment. At reattachment the pressure falls dramatically towards its steady value. The steady pressures are shown in Fig. 7 for varying geometry.

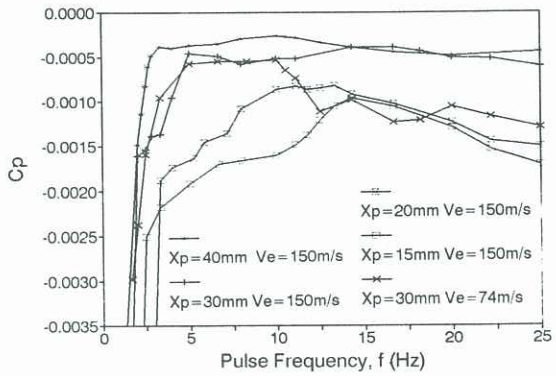

Fig. 6 Surface pressure coefficients on the nozzle axis in a pulsed flow with varying nozzle geometry, X_p and exit velocity V_e.

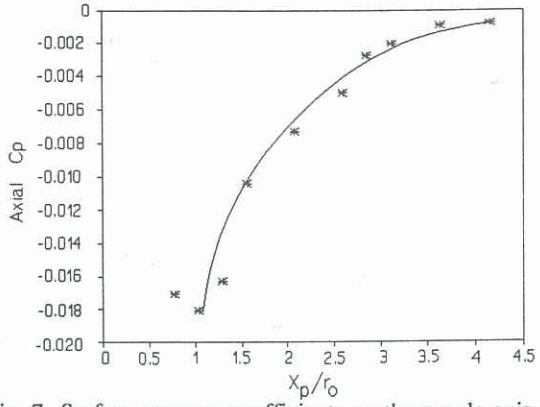

Fig. 7 Surface pressure coefficients on the nozzle axis as a function of X_p for steady RJR flow, V_e=150m/s.

As the mean exit velocity through the nozzle is increased from 74m/s to 150m/s (Fig.6), entrainment increases causing the flow to reattach more rapidly. Thus a stable flow results at a higher pulse rate as shown by the lower limiting frequency of 3Hz as compared to 5Hz for the higher velocity case.

The amount of fluid beneath the nozzle increases proportionally with X_p. A smaller volume will be entrained more rapidly for a given pulse frequency resulting in a higher limiting frequency as demonstrated in Fig. 6 for V_e=150m/s.

Flow Development The measured and computed flow fields for a developing pulse showed a reasonable correlation (Fig. 8). The computed flow was for the case of a developing flow to its steady state while the experimental results were taken for a full cycle of a pulsing flow at 25Hz with a 1:2 on/off ratio. The pulse reached its peak velocity at the nozzle outlet in a time of 6.6 ms. The peak velocity was observed at varying times depending on the location of the point in interest. The experimental values decayed after their peak velocity while the modelled results converged to a steady state value as indicated by the divergence of the three curves (Fig. 8) at times of 11, 18 and 11 ms onwards for z = 9, 15 and 25 mm respectively.

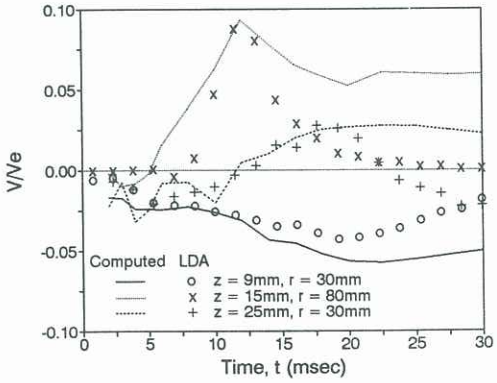

Fig. 8 Radial velocity components during flow development.

Reynolds Shear Stress.

Reynolds shear stress is of interest as it is directly

related to the turbulent heat and mass transfer rates. The comparison between computed and experimental Reynolds shear stress was unexpectedly poor (Fig. 9). The modelled Reynolds shear stress was obtained from Eq. (1)

$$\overline{uv} = -0.09\frac{k^2}{\varepsilon}\left(\frac{\partial U}{\partial y}+\frac{\partial V}{\partial x}\right) \qquad (1)$$

$\overline{uv}$ is dependant on the turbulent kinetic energy, k, the dissipation, ε, and the velocity gradients. The modelled results greatly underpredict the experimental values (Fig. 9). Some disagreement of the location of peaks in the curves is also noted.

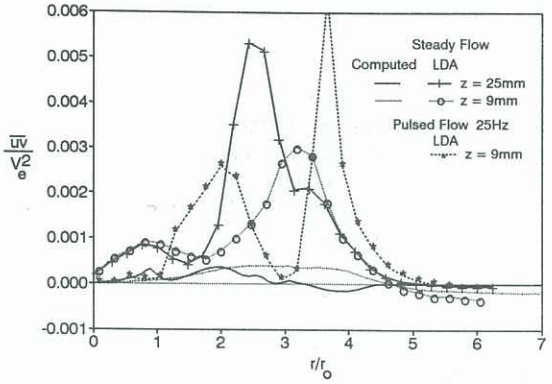

Fig. 9 Reynolds shear stress for steady and pulsed flow.

With pulsing at 25 Hz, the mean aggregate shear stress (Fig. 9) for z = 9mm is greatly increased. The maxima occur further out in the flow at 2 and 4 r_o indicating a smaller curvature of the radial jet due to incomplete reattachment. As shown, pulsing the jet above the limiting frequency of 5Hz (Fig. 6) has improved the potential of the jet for transfer operations.

An underprediction is also noted in a comparison of turbulent kinetic energy, k (Fig. 10). The measured k is calculated using only the u and v velocity components. The maxima of k (Fig. 10) occurring between 2.5 and 3.5 r_o coincide with the position of the high turbulence associated with the surface vortex. These peaks in k, influence the shear stress as seen in Fig. 9. The minor peak occurring between 1 and 2 r_o (Fig. 9), is associated with the high velocity gradients generated by the surface vortex.

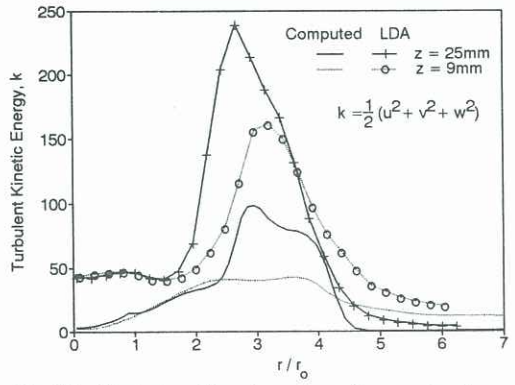

Fig 10. Turbulent kinetic energy for steady flow.

Unfortunately, measurement of dissipation is not readily possible to complete the comparison between measurements and prediction. However, flow visualisation data provided by the video recording of flow provide a likely explanation for the mismatch between experimental and prediction, at least for the steady flow case. From the videos it is clearly seen that a steady reattachment curtain does not exist due to periodic blowouts that do not even occur axisymmetrically. This aspect of the flow is quite dominant and would add considerably to measured turbulence levels later including k and $\overline{uv}$. The k-ε model is a steady state one which cannot account for such additional features of the flow. The latter adds a second time scale and possibly other length scales. Consequently, the observed disagreement can be expected. Such disagreement was also observed by Graham and Bremhorst (1992) when applying the k-ε model to a fully pulsed jet.

CONCLUSIONS

Comparisons between numerical and experimental results have shown the standard form of the k-ε model to produce acceptable mean velocity predictions within highly turbulent and unstable flows of an RJR flow field. However, due to the inherent limit of one time scale and one length scale, there is a significant error in the prediction of turbulent kinetic energy, k, and Reynolds shear stress. Using the numerical results to predict heat transfer from the Reynolds shear stress is likely to lead to significant error.

The industrial benefits of pulsing the RJR jet are evident in the increased Reynolds shear stress over that of steady flow. The transition from steady reattached to unsteady non-reattached is given by a limiting frequency which depends on flow geometry and exit velocity.

REFERENCES

AGNEW, N D, (1991), An investigation of the radial jet reattachment (RJR) flow field using laser Doppler anemometry and flow visualisation. Undergraduate Thesis, University of Queensland, Brisbane, Qld.

BREMHORST, K and FLINT, P J, (1991) The effect of flow patterns on the erosion-corrosion of shell and tube heat exchangers. Wear, *145*, 123-135.

ELVERY, D G, (1991) Computer simulation of turbulent flow in impinging jets. Undergraduate Thesis, University of Queensland, Brisbane, Qld.

GRAHAM, L J W and BREMHORST K, (1992), Application of k-ε turbulence model to the simulation of a fully pulsed free air jet, J. Fluids Engineering, ASME, to appear.

PAGE, R H and KIEL, R (1990), Utilization of radial jet reattachment (RJR) for industrial drying. Proc of Forum on Industrial Applications of Fluid Mechanics, ASME, FED, *100*.

WINTER, A R, GRAHAM, L J W and BREMHORST, K, (1991) Effects of time scales on velocity bias in LDA measurements using sample and hold processing. Experiments in Fluids, *11*, 147-152.